Electronic Supplementary Material (ESI) for Journal of Materials Chemistry A.
This journal is © The Royal Society of Chemistry 2022

Supplementary materials for

Evaluation of N-doped carbon for the peroxymonosulfate activation and removal of organic contaminants from livestock wastewater and groundwater

Shu Cai[a], Xiaoxue Zuo[b], Haiyan Zhao[b], Shengjiong Yang[c], Rongzhi Chen[d], Liwei Chen[b], Ruihong Zhang[a], Dahu Ding[b,*], Tianming Cai[b,*]

[a] Department of Biological and Agricultural Engineering, University of California, Davis, CA, 95616, United States

[b] College of Resources and Environmental Sciences, Nanjing Agricultural University, Nanjing 210095, China

[c] Key Laboratory of Environmental Engineering, Xi'an University of Architecture and Technology, Xi'an 710055, China

[d] College of Resources and Environment, University of Chinese Academy of Sciences, Beijing 101408, China

This information contains:

4 Texts

4 Tables

25 Figures

Text S1. Detection of antibiotics in livestock wastewater (LW)

Antibiotics were identified using liquid chromatography with tandem mass spectrometry (HPLC-MS/MS), consisting of an Agilent 1200 series HPLC coupled to a 6410 triple quadrupole mass spectrometer (Agilent Technologies, USA). Separation was accomplished using an Agilent ZORBAX Eclipse Plus C18 column (3.5 μm, 2.1 mm × 150 mm). Elution was performed at a flow rate of 0.2 mL min^{-1}, consisting 60% A (H_2O with 0.1% acid) and 40% B (Methanol). Quantitative analysis was adopted, and the detection mode was MRM model. Mass spectral analysis was conducted in both positive and negative mode using an electrospray ionization (ESI) source. Instrument parameters were as follows: drying gas flow 10 L min^{-1}, temperature 330 °C, Atomizer pressure 30 psi, Capillary voltage 35 kV and nitrogen (≥ 99.999%) was used as cone and collision gas. Mass analyzer was operated in full scan mode (*m/z* range 50−1000) in order to identify the products.

Text S2. Detection of petroleum hydrocarbons in groundwater (GW)

Petroleum hydrocarbon were identified using Gas Chromatography/Mass Spectrometry (Bruker 320-MS). The experimental conditions were as follows: the inlet temperature was 320 ℃, and the column flow rate was 1.2mL min^{-1}. The initial temperature of the column was kept at 60 ℃ for 1 minute, increased to 290 ℃ at 8 ℃ min^{-1}, and then heated to 320 ℃ at 30 ℃ min^{-1}, and kept for 7 minutes. The injection method adopts non-split injection, which is separated 0.8 minute later with a split ratio of 20:1 and an injection volume of 1 μL. All samples were extracted with dichloromethane and concentrated with n-hexane, purified with magnesium silicate, then concentrated with nitrogen blowing, and finally condensed with n-hexane to 1.0 mL.

Text S3. Detailed detection methods of SMX transformation products (TPs).

Degradation intermediates and TPs were identified using liquid chromatography with tandem mass spectrometry (HPLC-MS/MS), consisting of an Agilent 1200 series HPLC coupled to a 6410 triple quadrupole mass spectrometer (Agilent Technologies, USA). Separation was accomplished using an Agilent ZORBAX Eclipse Plus C18 column (3.5 μm, 2.1 mm × 150 mm). Elution was performed at a flow rate of 0.25 mL min^{-1}, consisting 60% A (H_2O) and 40% B (Methanol). Mass spectral analysis was conducted in both positive and negative mode using an electrospray ionization (ESI) source. Instrument parameters were as follows: drying gas flow 10 L min^{-1}, temperature 330 °C, Atomizer pressure 30 psi, Capillary voltage 35 kV and nitrogen (≥ 99.999%) was used as cone and collision gas. Mass analyzer was operated in full scan mode (*m/z* range 50−1000) in order to identify the products.

Text S4. Details of density functional theory (DFT) calculations

The geometry optimization of SMX were firstly simulated by the DFT method. Fukui functions were chosen to describe the activity of orbital-controlled reactions, which indicated the larger value of the Fukui function, the higher reactivity of the corresponding site. The functions were listed as following:

Nucleophilic reaction: $$f^{+} = q_{N}^{A} + q_{N+1}^{A} \quad (1)$$

Electrophilic reaction: $$f^{-} = q_{N-1}^{A} + q_{N}^{A} \quad (2)$$

Radical reaction: $$f^{0} = (q_{N-1}^{A} + q_{N+1}^{A})/2 \quad (3)$$

where q_A is the electron population of atom A in the molecule. f^+ is used when the system undergoes a nucleophilic attack, whereas f^- is valid when the system undergoes an electrophilic attack. f^0 is used to govern the radical attacking reactions. The DFT calculations on $q_A(N)$, $q_A(N-1)$ and $q_A(N+1)$ were carried out in Gaussian 09, using the method of B3LYP/6-31+G** in combination with the SMD solvent model.

Table S1 Conditions for HPLC detection of organic contaminants.

Compounds	Ultrapure water	Acetic acid	Acetonitrile	Methanol	Flow rate (mL/min)	Wavelength (nm)
SMX		60%		40%	1.0	270
SDZ		75%	25%		1.0	268
OFL		63%		37%	1.0	278
BPA	30%			70%	1.0	227
PHE	30%			70%	1.0	270

Table S2. The deconvolution results of C 1s XPS spectra.[a]

Samples	C-C/C＝C	C-O	N-C＝N/O-C＝0
PDA-gCN-0.5	54.24	32.50	0.00
PDA-gCN -1.0	50.14	32.01	3.65
PDA-gCN -1.5	54.48	33.65	0.17

[a] The data given in the table were at%.

Table S3. Mass spectra data and proposed structures of identified transformation products of SMX.

	Compound	Molecular structure	Molecular weight	MS (*m/z*)	MS-MS (*m/z*)
	Sulfamethoxazole (SMX)	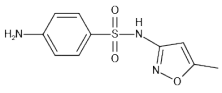	253	253.7 $[M+H]^+$ 275.9 $[M+Na]^+$	155.3$[M+H-C_4H_6N_2O]^+$ 108.3$[M+H-C_4H_6N_2O-SO]^+$
TP 1	3-amino-5-methyl-isoxazole (AMI)	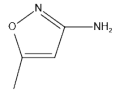	98	99.0 $[M+H]^+$	71.8$[M+H-CCH_2]^+$
TP 2	5-methyl-3-[2-(5-methyl-1,2-oxazol-3-yl)diazen-1-yl]-1,2-oxazole	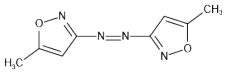	192	192.8 $[M+H]^+$	99.4$[M+H-C_4H_3N_2O]^+$
TP 3	4-sulfonylphenol	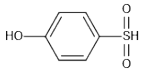	158	158.9 $[M+H]^+$	57$[M+H-C_3O_2]^+$
TP 4	4-Hydroxybenzenesulfonic acid	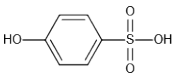	173	173.8$[M+H]^+$	NA[b]
TP 5	Monohydroxylated sulfanilic acid (OH-SAA)	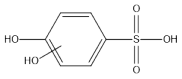	190	190.8 $[M+H]^+$ 212.7 $[M+Na]^+$	158.9$[M+H-NH_2O]^+$ 173.8$[M+H-NH_2]^+$
TP 6	Monohydroxylated sulfamethoxazole (OH-SMX)[a]	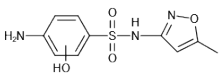	269	291.9 $[M+Na]^+$	NA
TP 7	Dimer	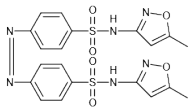	502	500.5 $[M-H]^-$	172.6$[M+H-C_4H_{13}NO]^+$

[a] Hydroxylation at aniline moiety, [b] not available.

Table S4. Estimated acute and chronic toxicity of SMX and its intermediate products using ECOSAR program.[a]

Compounds	Acute toxicity (mg L^{-1})			Chronic toxicity (ChT, mg L^{-1})		
	Fish (LC_{50})	Daphnia (LC_{50})	Green algae (EC_{50})	Fish	Daphnia	Green algae
SMX	267	6.43	21.8	5	0.068	11.1
TP1	270	3.63	13.8	6.59	0.036	9.16
TP2	326	179	117	30.7	16.0	28.5
TP3	1.07E+3	151.93	85.61	82.3	10.8	101
TP4	7.62 E+4	6.46E+3	5.84E+3	5.21E+3	368.63	5.21E+3
TP5	2.92 E+4	1.18E+6	989	3.01E+4	5.66 E+5	72
TP6	584	9.08	33.5	13.3	0.092	20.9
TP7	26.5	22.4	4.52	0.52	5.22	4.34

[a] According to the system established by the Globally Harmonized System of Classification and Labeling of Chemicals (United Nations, 2011), the four levels include: very toxic ($LC_{50}/EC_{50}/ChT$ < 1 mg L^{-1}), toxic (1 mg L^{-1} < $LC_{50}/EC_{50}/ChT$ < 10 mg L^{-1}), harmful (10 mg L^{-1} < $LC_{50}/EC_{50}/ChT$ < 100 mg L^{-1}), and not harmful ($LC_{50}/EC_{50}/ChT$ > 100 mg L^{-1}).

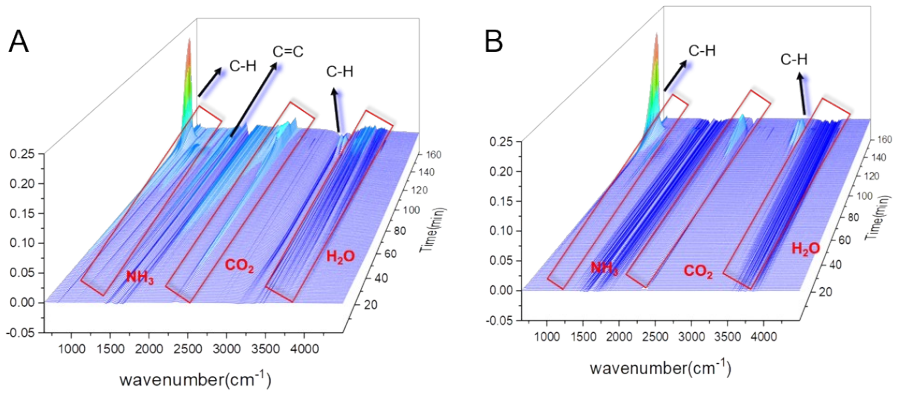

Fig. S1 TG-FT-IR spectra of g-C_3N_5 (A) and PDA@g-C_3N_5 (B).

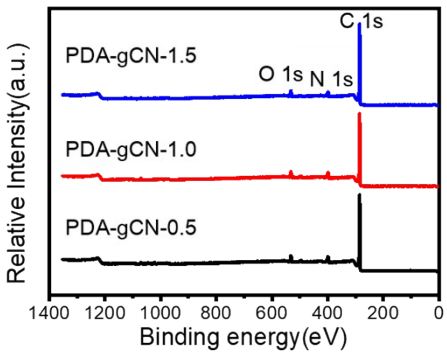

Fig. S2. XPS survey scan of PDA-gCN catalysts.

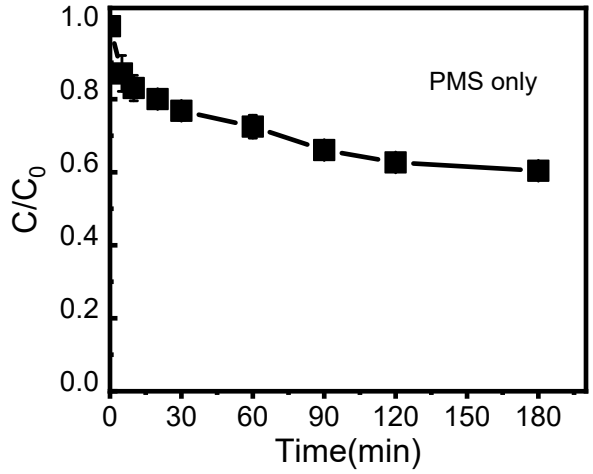

Fig. S3. Oxidation of SMX by unactivated PMS (Reaction conditions: [SMX] = 10 mg L^{-1}, [PMS] = 1 mM, initial pH = 5.32)

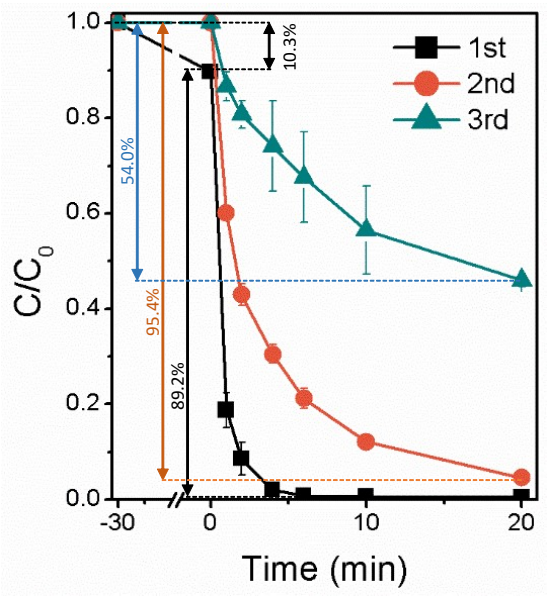

Fig. S4. Successive oxidation of SMX by using recycled PDA-gCN-1.0 catalyst. (Reaction conditions: [SMX] = 10 mg L^{-1}, [PDA-gCN-1.0] = 50 mg L^{-1}, [PMS] = 1 mM, initial pH = 5.32)

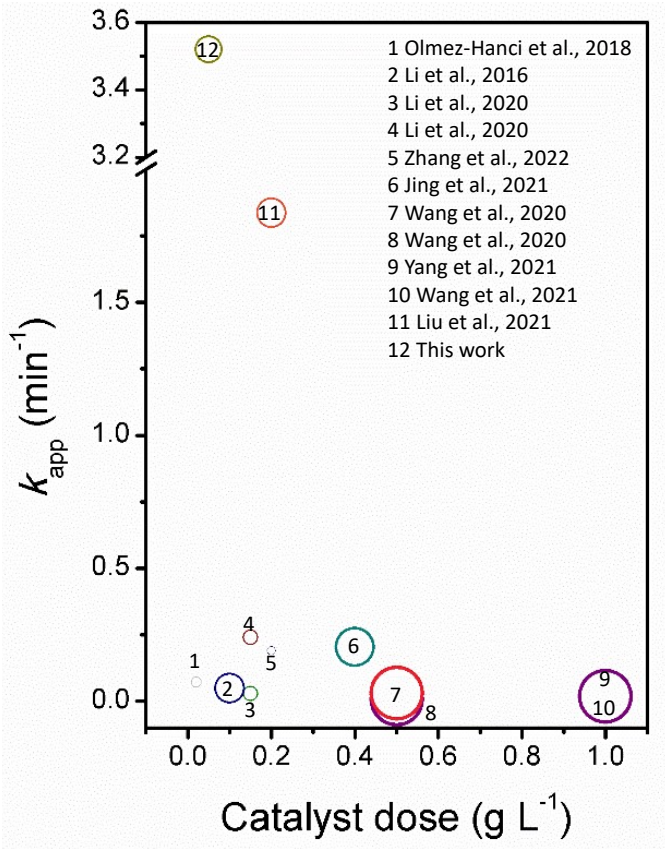

Fig. S5. Comparisons of BPA oxidation by PMS activated with PDA-gCN-1.0 and previously reported catalysts. (the diameter of the circles indicates the [BPA]/[PMS] ratio, the references are given in the Reference section)

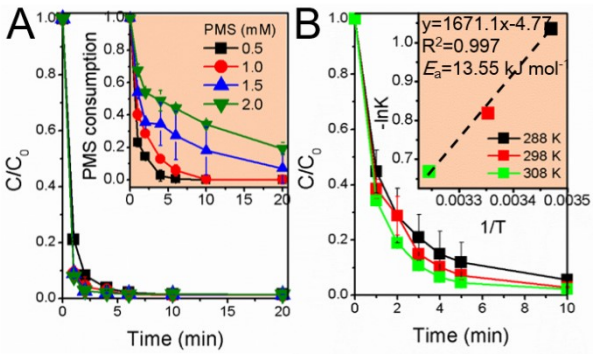

Fig. S6. Effects of PMS concentration (**A**) and reaction temperature (**B**) on catalytic oxidation of SMX by PDA-gCN-1.0/PMS process. (inset figure in **A** shows the corresponding PMS consumption profiles and inset figure in **B** shows the plot between 1/T and –ln*k*, Reaction conditions: [SMX] = 10 mg L^{-1}, [PDA-gCN-1.0] = 50 mg L^{-1}, [PMS] = 1 mM, initial pH = 5.32)

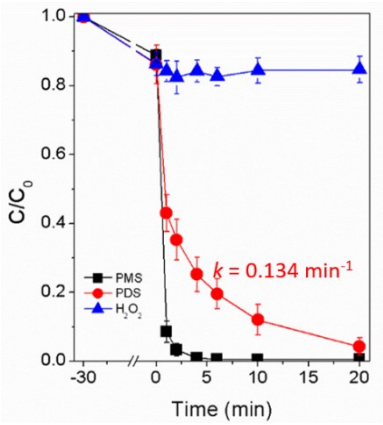

Fig. S7. Catalytic oxidation of SMX by PDA-gCN-1.0/PMS, PDA-gCN-1.0/PDS, and PDA-gCN-1.0/H_2O_2 processes. ([PMS] = [PDS] = [H_2O_2] = 1 mM, [SMX] = 10 mg L^{-1}, [PDA-gCN-1.0] = 50 mg L^{-1}, T=25 °C)

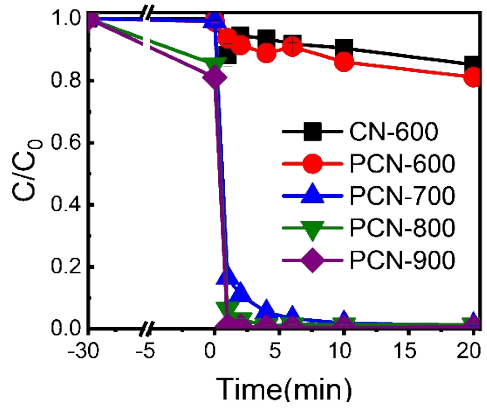

Fig. S8. Catalytic oxidation of SMX by PMS activated by different catalysts. (Reaction conditions: [SMX] = 10 mg L^{-1}, [PMS] = 1 mM, [catalyst] = 50 mg L^{-1}, T = 25 °C, initial pH = 5.32)

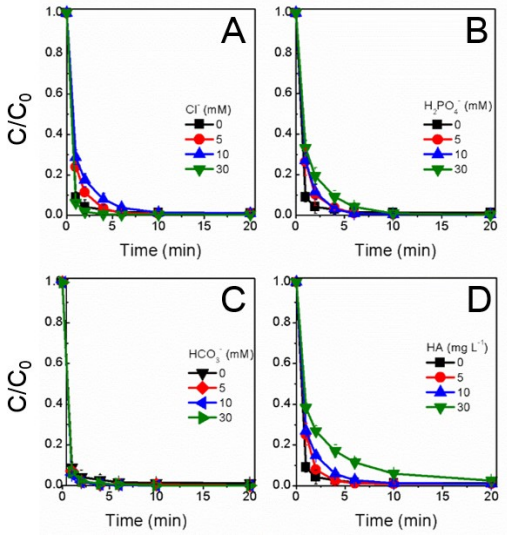

Fig. S9. Effects of coexisting substances (**a**: Cl^-, **b**: $H_2PO_4^-$, **c**: HCO_3^-, and **d**: HA) on SMX oxidation by PDA-gCN-1.0/PMS process. ([SMX] = 10 mg L^{-1}, [PMS] = 1 mM, [PDA-gCN-1.0] = 50 mg L^{-1}, pH = 5.32)

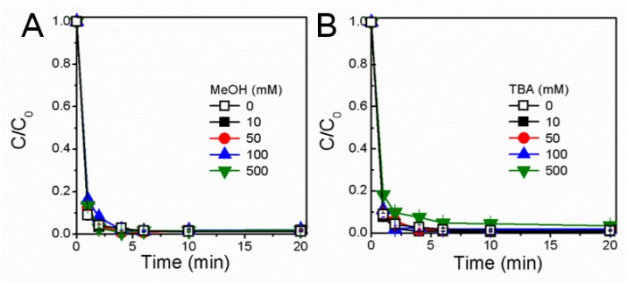

Fig. S10. Effects of ROS quenching agents (**a**: MeOH, **b**: TBA) on SMX oxidation process. ([SMX] = 10 mg L^{-1}, [PMS] = 1 mM, [PDA-gCN-1.0] = 50 mg L^{-1}, pH = 5.32)

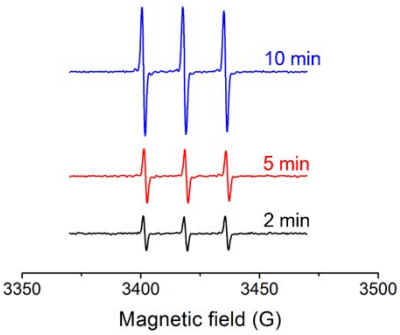

Fig. S11. EPR signals of $^1O_2$ using TEMP as trapping agent. ([SMX] = 10 mg L^{-1}, [PMS] = 1 mM, [PDA-gCN-1.0] = 50 mg L^{-1}, pH = 5.32)

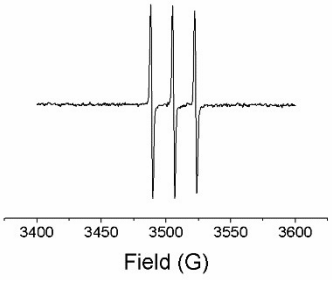

Fig. S12. EPR signals of $^1O_2$ in PMS solution without catalyst.

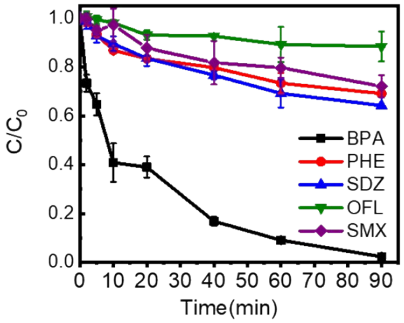

Fig. S13. Degradation of organic compounds by the UV/RB process. ([BPA] = [PHE] = [SDZ] = [OFL] = [SMX] = 5 mg L^{-1}, [RB] = 0.5 mM)

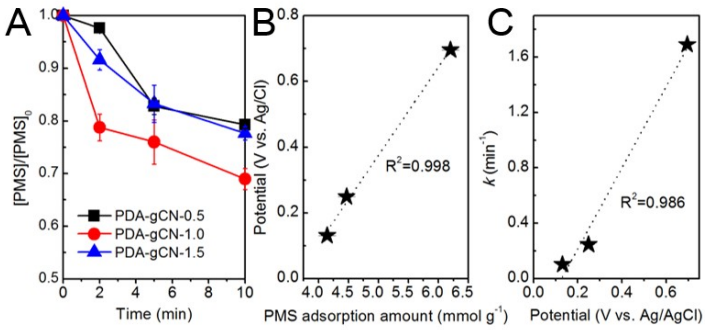

Fig. S14. Adsorption of PMS by PDA-gCN catalysts (A); correlation between the potentials of surface complexes and PMS adsorption amounts (B); correlation between *k* values and the potentials of surface complexes (C). ([PMS] = 1 mM, [catalyst] = 50 mg L^{-1}; T = 25 °C)

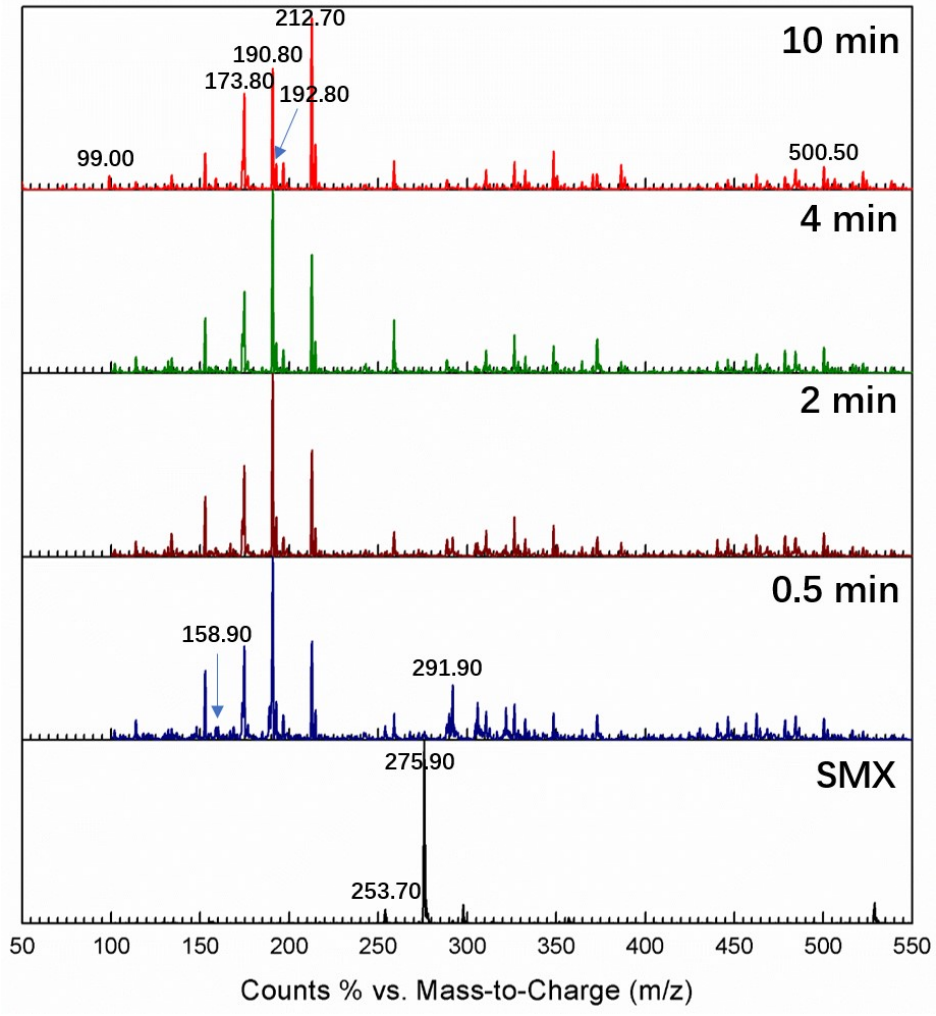

Fig. S15. Identification of SMX degradation product detected by Agilent Ultivo LC/MS/MS.

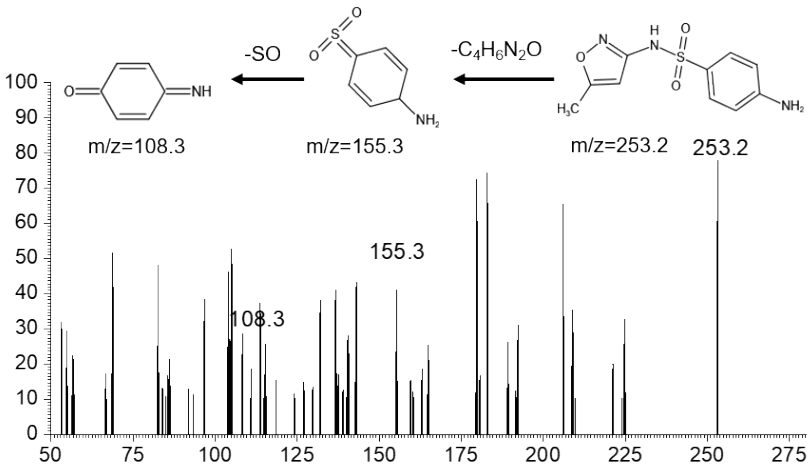

Fig. S16. Identification of SMX and its fragment ion 155 and 108.

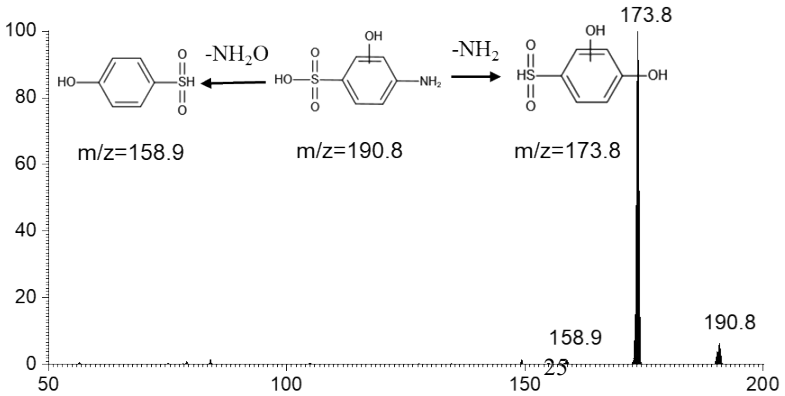

Fig. S17. Identification of SMX degradation product (m/z = 190.8) and its fragment ion 173.8 and 158.9.

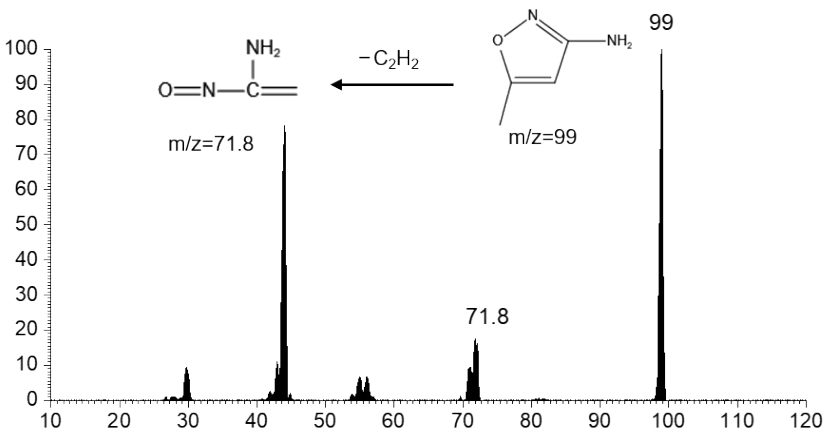

Fig. S18. Identification of SMX degradation product (m/z = 99) and its fragment ion 72.

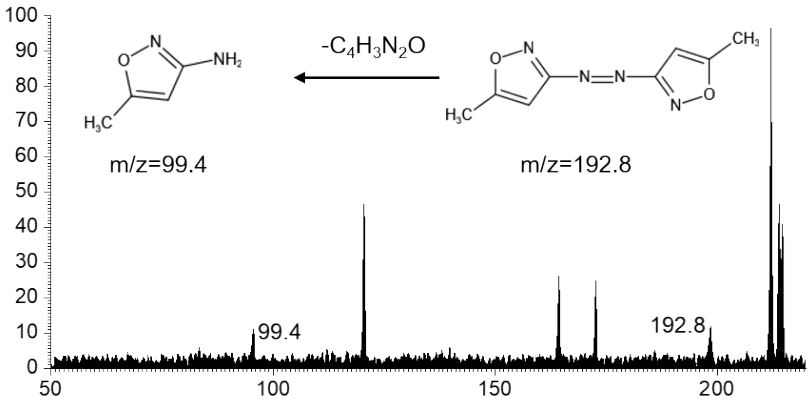

Fig. S19. Identification of SMX degradation product (m/z = 193) and its fragment ion 101.

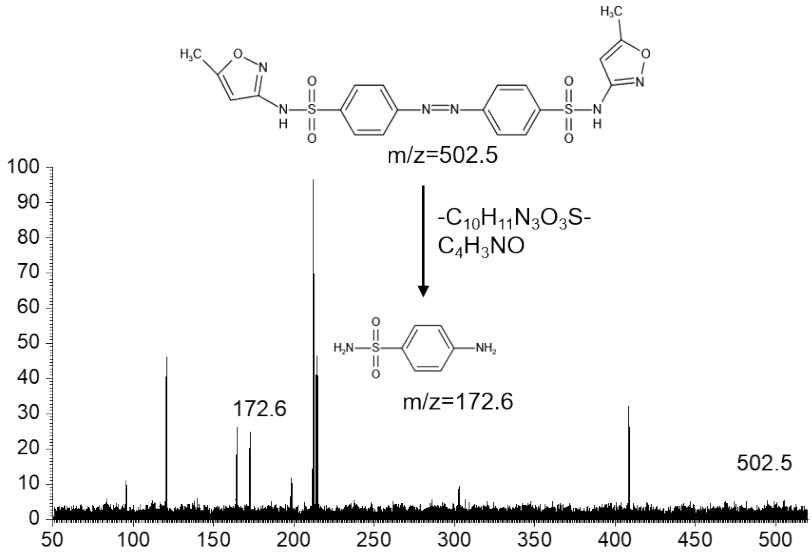

Fig. S20. Identification of SMX degradation product (m/z = 503) and its fragment ion 212 and 173.

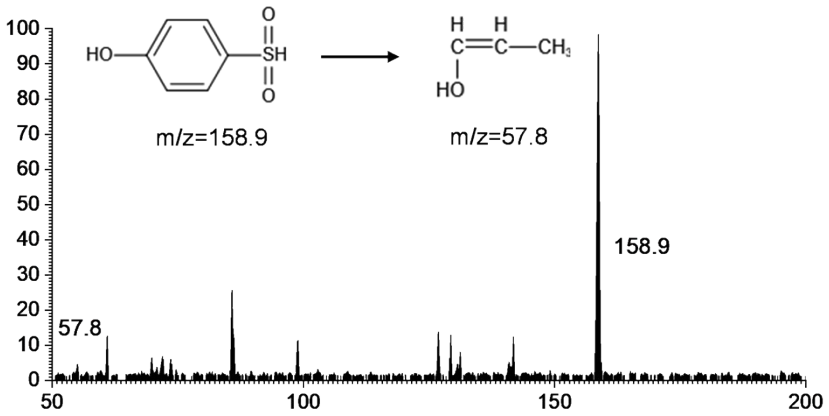

Fig. S21. Identification of SMX degradation product (m/z = 159) and its fragment ion 58.

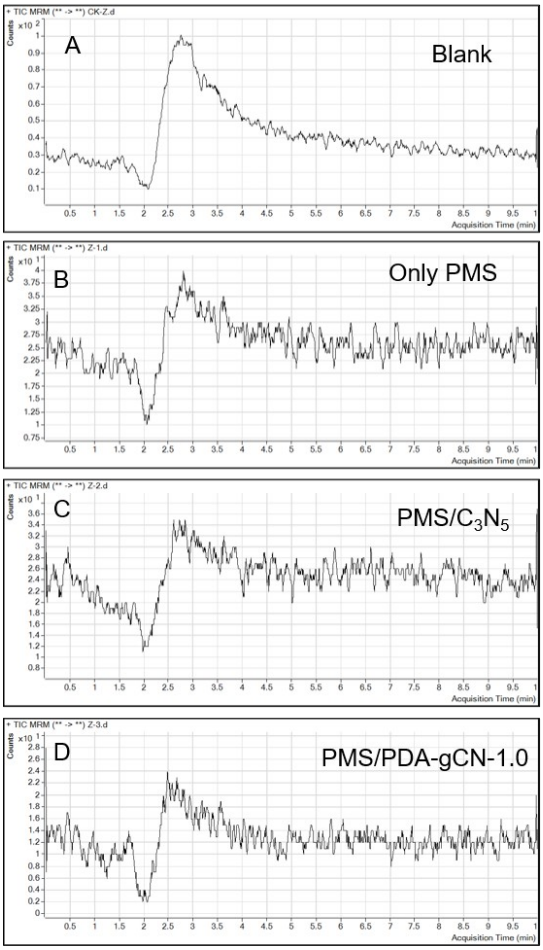

Fig. S22. LC-MS spectra of LW before and after AOPs treatment, blank (A), only PMS (B), PMS/C_3N_5 (C), PMS/PDA-gCN-1.0 (D).

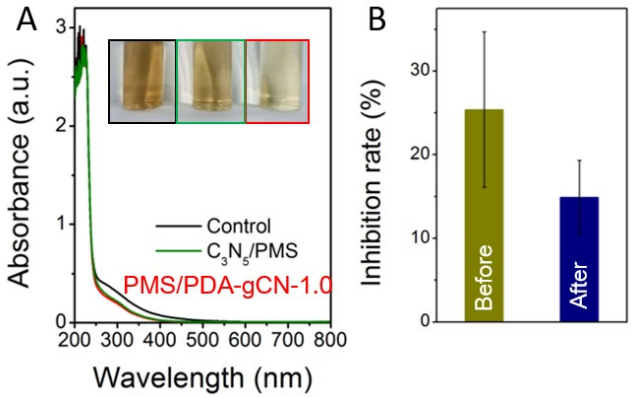

Fig. S23. UV spectra (a) and the inhibition rates of *E. coli* (b) of the LW samples before and after AOPs treatment (inset figures show the photographs of raw and treated LW samples).

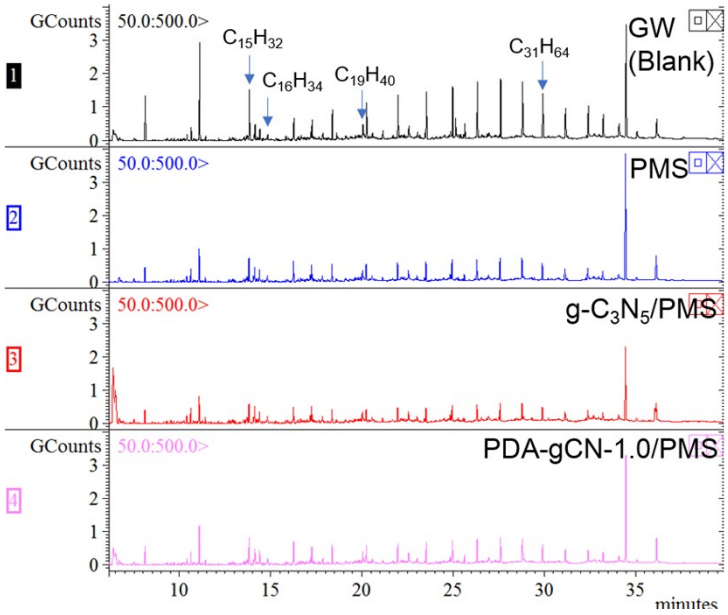

Fig. S24. GC-MS spectra of GW samples before and after AOPs treatment, only PMS (A), C_3N_5 /PMS (B), PDA-gCN-1.0/PMS (C).

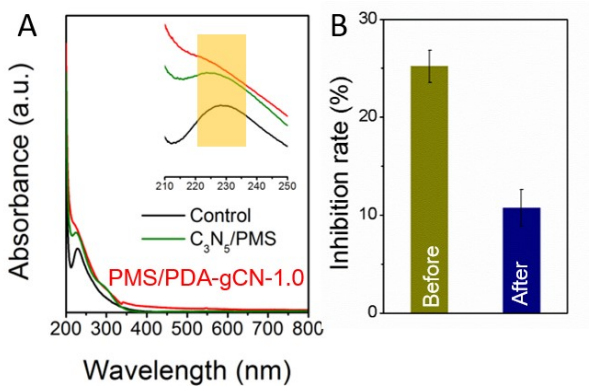

Fig. S25. UV spectra (a) and the inhibition rates of *E. coli* (b) of the GW samples before and after AOPs treatment (inset figures show the photographs of raw and treated LW samples).

References

1. Z. Zhang, H. Ding, Y. Li, J. Yu, L. Ding, Y. Kong and J. Ma, *Sep. Purif. Technol.*, 2022, **283**, 120136.
2. Z. Yang, Z. Wang, G. Liang, X. Zhang and X. Xie, *Chem. Eng. J.*, 2021, **426**, 131777.
3. Y. Li, T. Yang, S. Qiu, W. Lin, J. Yan, S. Fan and Q. Zhou, *Chem. Eng. J.*, 2020, **389**, 124382.
4. J. Jing, M. N. Pervez, P. Sun, C. Cao, B. Li, V. Naddeo, W. Jin and Y. Zhao, *Sci. Total. Environ.*, 2021, **801**, 149490.
5. X. Li, Z. Wang, B. Zhang, A. I. Rykov, M. A. Ahmed and J. Wang, *Appl. Catal. B: Environ.*, 2016, **181**, 788-799.
6. N. Liu, N. Lu, H. Yu, S. Chen and X. Quan, *Chem. Eng. J.*, 2021, **407**, 127228.
7. H. Wang, W. Guo, B. Liu, Q. Si, H. Luo, Q. Zhao and N. Ren, *Appl. Catal. B: Environ.*, 2020, **279**, 119361.
8. H. Wang, W. Guo, Q. Si, B. Liu, Q. Zhao, H. Luo and N. Ren, *Chem. Eng. J.*, 2021, **418**, 129504.
9. T. Olmez-Hanci, I. Arslan-Alaton, S. Gurmen, I. Gafarli, S. Khoei, S. Safaltin and D. Yesiltepe Ozcelik, *J. Hazard. Mater.*, 2018, **360**, 141-149.